Physical Phenomena Facilitating the Penetration of Solutions of TiO₂ Nanoparticles through Protective Gloves

Ludwig Vinches, Jessy de Santa Barbara, Stéphane Hallé
École de Technologie Supérieure
1100 Notre-Dame Ouest, Montréal QC H3C 1K3 Canada
ludwig.vinches@mail.mcgill.ca

Patricia Dolez
CTT Group
3000 rue Boullé, Saint-Hyacinthe QC J2S 1H9 Canada

Kevin J. Wilkinson
Dept. De chimie, Université de Montréal
C.P. 6128, succ. Centre-ville, Montréal QC H3C 3J7 Canada

Abstract– *Titanium dioxide nanoparticles (nTiO₂) are found in numerous manufactured products such as sunscreens and paints. Nevertheless, some studies have expressed concern about their likely harmful effects on health. Application of the precautionary principle has led to the recommendation for the use of protective gloves by numerous Health & Safety agencies. However, recent work has shown that solutions of nTiO₂ can penetrate the protective materials of gloves under conditions simulating occupational use.*
This study has been designed to identify some of the physical phenomena that may facilitate the penetration of nTiO₂ through elastomer membranes subjected to mechanical deformations (such as those produced by flexing the hand).
Nitrile rubber and latex gloves were brought into contact with two solutions of nTiO₂. Mechanical deformations were applied to samples of protective gloves during their exposure to nanoparticles. Repetitive mechanical deformations affected both the physical and mechanical properties of protective materials. Moreover, the elastomers used in protective gloves were also shown to be sensitive to the action of the nTiO₂ solutions. Elastomer swelling was observed, leading to a modification of the mechanical and chemical properties of the gloves.

Keywords: TiO₂ nanoparticles, protective gloves, mechanical deformation, occupational use.

1. Introduction

Titanium dioxide nanoparticles (nTiO₂) are increasingly present in commercial products such as paints, varnishes, sunscreens, etc. [1, 2]. The global production of nTiO₂ was 50,400 tons in 2010 and is expected to reach 201,500 tons in 2015 (Future Markets 2011). As a result, the exposure of workers and researchers to nTiO₂ is expected to rapidly increase. At the same time, an increasing number of studies are expressing concern about the likely harmful effects of nTiO₂ on human health. For example, a small increase in the number of cancers among workers who were in contact with nTiO₂ has been reported [3]. Moreover, for studies conducted by intratracheal instillation of rats and mice to 250 nm TiO₂ pigments and 20 nm nTiO₂, inflammation of the lungs was higher for the nanoparticulate form of TiO₂ [4-6]. Following these results, the International Agency for Research on Cancer (IARC) classified

nanosized titanium dioxide as being possibly carcinogenic to humans (i.e. 2B group, [7]). In response to this classification, several government agencies responsible for the health and safety of workers have recommended application of the precautionary principle [8, 9]. One of their recommendations is the use of protective gloves and clothing when working with nanoparticles, even though no scientific validation of their efficiency has yet been made.

A limited number of groups have reported research on the use of protective gloves for nanoparticles. Much of the research has involved nanoaerosols and, in some cases, conflicting results have been found. Diffusion of 30 and 80 nm graphite nanoparticles through nitrile, vinyl, latex and neoprene commercial glove samples has been reported [10], while no penetration was later measured for the same gloves when exposed to 40 nm graphite, 10 nm TiO_2 or 10 nm Pt particles [11, 12]. Nonetheless, under occupational settings, nanoparticles may be found as colloidal suspensions. This situation is especially relevant to protective gloves. For example, Vinches et al. exposed samples of nitrile, latex and neoprene gloves to $nTiO_2$ solutions in water while deforming the gloves by simulating flexing [13, 14]. Analyses by inductively coupled plasma mass spectrometry (ICP-MS) suggested that $nTiO_2$ was able to penetrate through the protective gloves when they were subjected to dynamic mechanical deformations for a period of 5 hours or more. In addition to mechanical deformation, the swelling of gloves materials might be facilitate the penetration of $nTiO_2$ solutions through protective gloves [15].

This paper reports analysis of some physical and mechanical phenomena which may facilitate the penetration of $nTiO_2$ solutions through nitrile rubber and latex protective gloves submitted to biaxial deformations. These results were obtained using commercial colloidal solutions of 15 nm $nTiO_2$ in water and in 1,2-propanediol.

2. Materials
2. 1. Protective Gloves
Three models of protective gloves corresponding to two types of elastomers were selected for this study: disposable 100 and 200 μm thick nitrile rubber gloves (identified as NBR-100 and NBR-200 respectively), and disposable 100 μm thick latex gloves. All samples were taken from back and palm sections of the gloves.

2. 2. Nanoparticles
TiO_2 nanoparticles have been chosen in this study because of their widespread use. The $nTiO_2$ (15 nm, anatase) was suspended in two solutions: water (15 wt%, Nanostructured & Amorphous Materials, Inc., Houston, TX) and in 1,2-propanediol, PG (20 wt%, MK Impex, Mississauga, ON).

3. Methods
3. 1. Characterization of the $nTiO_2$ solutions
A series of experiments were performed to characterize the nanoparticle solutions. First, the analysis of the $nTiO_2$ stock solution following dilution to 10 mg L^{-1} was performed by fluorescence correlation spectroscopy (FCS) in order to give the hydrodynamic diameter [16]. Second, thermogravimetric analysis (TGA, Diamond TGA/DTA Perkin Elmer) was used to evaluate the mass ratio of the $nTiO_2$ and identify the presence of additives in the colloidal solutions, aside from the liquid carrier. Gradual evaporation of the liquid carrier occurred between 25 and 150 ºC at a heating rate of 5°C/min. Finally, comparisons were made among the $nTiO_2$ carrier solutions and the technical grade and ultra-high purity solvents that were used as the liquid carriers by analysing spectra obtained using Fourier transform infrared spectroscopy (FT-IR, Nicolet Continuum XL). Measurements were made in attenuated total reflectance (ATR) mode, between 500 and 4000 cm^{-1}, on drops of solutions after near total solvent evaporation.

To obtain statistically significant data, triplicate measurements were performed for all analyses.

3. 2. Experimental Setup for the Mechanical Deformations
The test setup used for this study is illustrated in Figure 1. It includes an exposure chamber and a sampling chamber, which are separated by the glove sample. Both chambers and all elements that come in contact with the $nTiO_2$ are made of ultrahigh molecular weight polyethylene in order to limit the adsorption of $nTiO_2$ as documented by FCS. $nTiO_2$ are introduced into the exposure chamber, in direct contact with the external surface of the glove samples. The setup has been designed in order to expose the glove samples to colloidal solutions of $nTiO_2$, while simultaneously subjecting them to static or dynamic mechanical constraints. Indeed, the test setup was equipped with a probe linked to an electronic system for applying static or dynamic mechanical stress to the sample (Figure 1). The system is computer controlled and includes a 200-N load cell and a position detector. The whole system is enclosed in a

glove box to ensure operator safety during the assembly, dismounting and clean-up operations as well as during the tests. The time profile of sample deformations is illustrated in Figure 2a and involved applying a 50% deformation every minute. The probe head used in this study is shown in Figure 2b. It corresponded to a conical-spherical geometry that simulates biaxial deformations (BD) similar to that produced in gloves when flexing the hand [17].
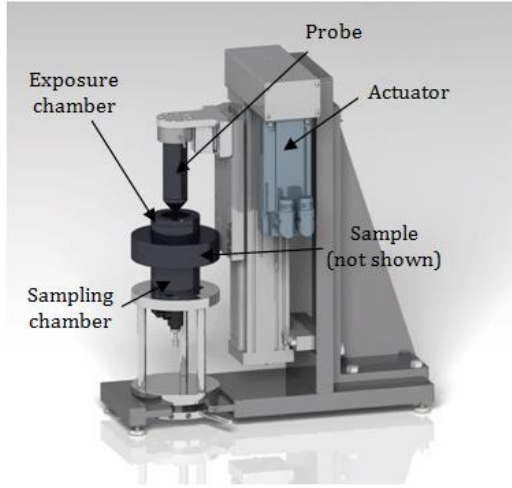

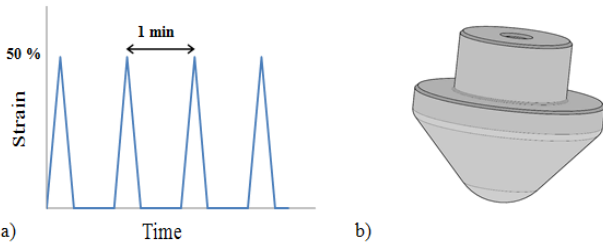Figure 1. Isometric view of the test setup.

Figure 2(a). Schematic representation of the variation of the sample deformation as a function of time during a dynamic deformation event and Figure 2(b) Illustration of the conical-spherical probe head.

3. 3. Quantification of the Characteristic Features on the Glove Surface

The surface morphology of five samples for each elastomer, was analysed by scanning electron microscopy (SEM, Hitachi S3600N – Vacc = 15 kV – magnification × 1000). Quantification of the surface area of the primary features (pores for nitrile and cracks for latex) was performed using image processing software (ImageJ).

3. 4. Strain Energy

Stress-strain curves, corresponding to the applied 50% dynamic deformation during tests, were plotted in order to follow the variation of the strain energy. An estimation of the relative strain energy was carried out by computing the area under the curves using the trapezoidal method.

3. 5. Determination of the Degree of Crystallinity

A semi-crystalline polymer is composed of crystallites dispersed in an amorphous matrix. Each of these two phases gives a particular diffraction signal [18]. X-ray diffraction profiles were obtained using a Pananalytical X'Pert Pro diffractometer in the scanning range of 2-50º and a Cu Kα radiation (45 kV, 40 mA). The degree of crystallinity (χ) was calculated as the ratio of the area under the crystalline peaks divided by the total area under all peaks in the diffraction profile [19], according to Eq. (1):

$$\chi = \frac{I_T - I_a}{I_T + I_B} \times 100 \tag{1}$$

with I_T being the area under the total intensity profile; I_a the intensity of the amorphous phase and I_B the area under the baseline profile.

3. 6. Length Change Measurements

Length change measurements were performed on 5 × 60 mm rectangular samples taken from the back or the palm section of the gloves. To obtain statistically significant data, three replicates were evaluated for each test. The measurements were performed by immersing the samples in the commercial nTiO$_2$ solutions. At regular intervals, samples were removed from the liquid, their surface gently wiped with a paper towel and lengths measured using a calliper (±0.01 mm). Length change data were computed using Eq. (2):

$$\Delta L(t) = \frac{L_t - L_0}{L_0} \tag{2}$$

with L_t being the length at time t and L_0 the corresponding length prior to immersion.

4. Results and Discussion
4. 1. Characterization of the nTiO$_2$ Solutions

FCS analyses were performed to measure the hydrodynamic diameter of the nTiO$_2$ in the two solutions. In water, the hydrodynamic diameter ranged from 19 nm to 23 nm, while in PG, the analysis was not possible due to an incompatibility between the FCS cells and the solvent.

The relative mass loss was measured as a function of temperature for the PG and for the PG containing nTiO$_2$ (Figure 3). In the presence of nTiO$_2$,

the curve was slightly shifted towards higher temperatures as compared to its absence. This observation can be attributed to the adsorption of solvent molecules by the nanoparticles, thus increasing the vapour pressure of the system [15]. In the case of $nTiO_2$ in water, the effect was also observed, but with a smaller amplitude. The calculated mass fraction obtained for $nTiO_2$ was 14.3 ± 0.8 % in water and 25.0 ± 3.7 % in PG. These results are in agreement with the manufacturer's indications.

FT-IR analyses were performed to see if additives, such as stabilizing agents, were present in the $nTiO_2$ solutions (Figure 4). A peak appearing at 1070 cm^{-1} in the water used to suspend the $nTiO_2$ was not observed in Milli-Q water (18.2 MΩ.cm of resistivity and Total Organic Carbon less than 1 µg.L^{-1}). This peak was associated with the elongation of a CO bond, likely indicative of a surfactant additive in the $nTiO_2$ solution. In contrast, the FTIR spectra of the PG used to suspend the $nTiO_2$ did not differ significantly from reagent grade PG. Nonetheless, spectra were admittedly complex, making the detection of additional peaks difficult.
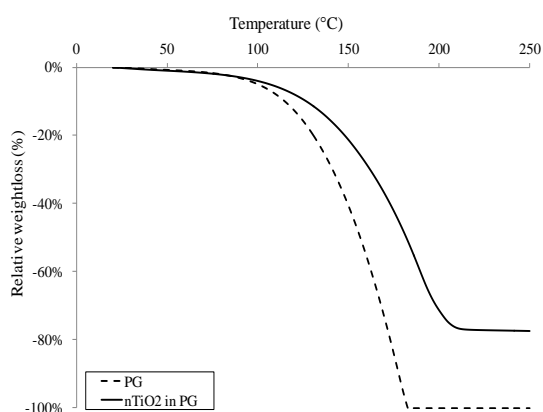

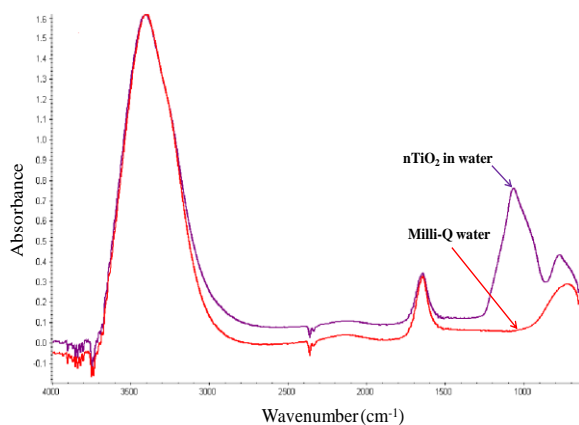Figure 3. TGA spectra of $nTiO_2$ in PG and ultra pure PG.

Figure 4. FT-IR spectra of $nTiO_2$ solution in water and of Milli-Q water.

4. 2. Characterization of the Surface of the Protective Gloves

Micrometer-size pores could be observed on the surface of the gloves (Figure 5), as already reported in the literature [20]. Indeed, micrometer-size pores were observed on both the inner and outer surfaces of both models of the nitrile glove. For the latex, micrometer-size cracks were seen on both surfaces.
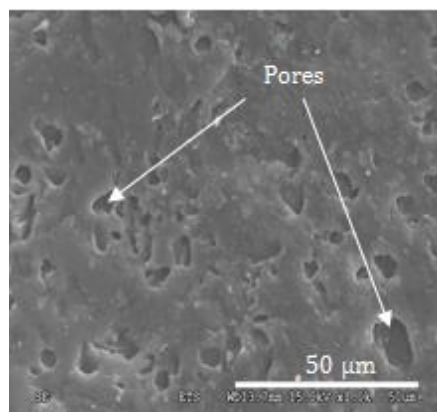

Figure 5. SEM image of the native outer surface of nitrile rubber glove (NBR-100).

4. 3. Swelling of Glove Materials in $nTiO_2$ Solutions

In order to investigate the cause of the $nTiO_2$ penetration through protective gloves, the swelling of nitrile rubber and latex was studied by recording the length change of samples after immersion in $nTiO_2$ solutions. Figure 6 displays a gradual length change increase for the two nitriles immersed in the aqueous $nTiO_2$, indicating significant diffusion of the $nTiO_2$ solution into the elastomer. A larger swelling ratio was recorded for NBR-100. For example, after 3 hours of immersion, the length change ratio for the NBR-100 was 4% whereas it was 2% for the NBR-200 (Table 1). It should be noted that maximum swelling was not attained for either of the two nitrile rubber gloves after 3 hours of immersion. For the NBR-100, a plateau was reached after 20 hours of immersion, with a maximum swelling of 9%. For the NBR-200, a maximum swelling of 12% was observed after 8 days of immersion. The difference in behaviour between the two models of nitrile rubber can be attributed to possible differences in the penetration of water, which may induce different affinities to the colloidal solution. According to the Table 1, the difference in swelling between NBR and latex glove may well the primary reasons that the aqueous $nTiO_2$ was able to more easily penetrate the NBR [21].
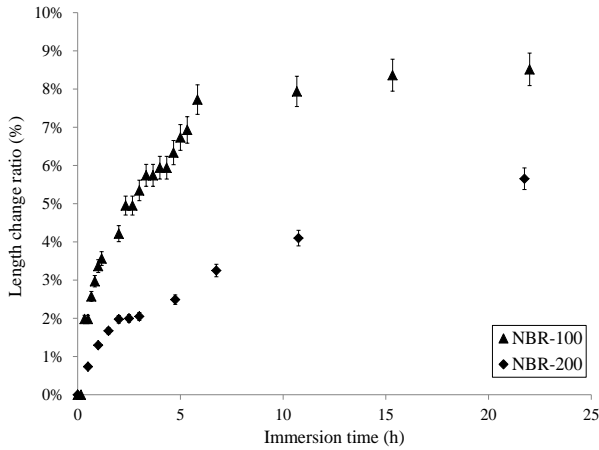
Figure 6. Length change ratio as a function of immersion time in aqueous $nTiO_2$ for the two nitrile rubber glove models.

The values of the length change ratio after 3 hours of immersion are provided in Table 1. The same tendency was observed for each of the $nTiO_2$ solutions: NBR-100 swelled more than NBR-200 and latex. A large difference was also observed between the $nTiO_2$ solutions: $nTiO_2$ in water induced swelling faster than the $nTiO_2$ in PG for all of the studied glove materials. This difference in swelling behavior produced by the two solutions can be attributed to differences in their ability to penetrate (diffuse) into the elastomer.

Table 1. Values of the length change ratio after 3 hours of immersion of the glove materials in the $nTiO_2$ solutions.

	Length change ratio after 3 hours (%)	
	$nTiO_2$ in water	$nTiO_2$ in PG
NBR-100	4.0	2.8
NBR-200	2.0	0.2
Latex	1.7	0.3

4. 4. Effect of the Mechanical Deformations and the Ntio₂ Solutions on the Gloves

The sample glove surface morphology was first characterized following exposure to the dynamic biaxial deformations (BD) in the absence of the $nTiO_2$ solutions. Figure 7 displays the variation of the surface features as a function of the number of deformations for NBR-100. While no significant effect was recorded on the inner surface, the outer surface appeared to be strongly affected by the mechanical deformations. Indeed, an increase in the surface area attributed to the pores was observed after only 30 BD, increasing by more than three-fold after 180 BD. The same observations could be made for the outer surface of the latex glove. In contrast, NBR-200 was

much less affected than either the NBR-100 or latex. In those cases, the deterioration of the materials could be attributed to an abrasion of the sample surface by the probe [22]. This hypothesis was supported by the observation of a reduction in surface features when the mechanical deformations were performed in the presence of the $nTiO_2$ solutions (see Figure 8), which might have played the role of a lubricating agent.
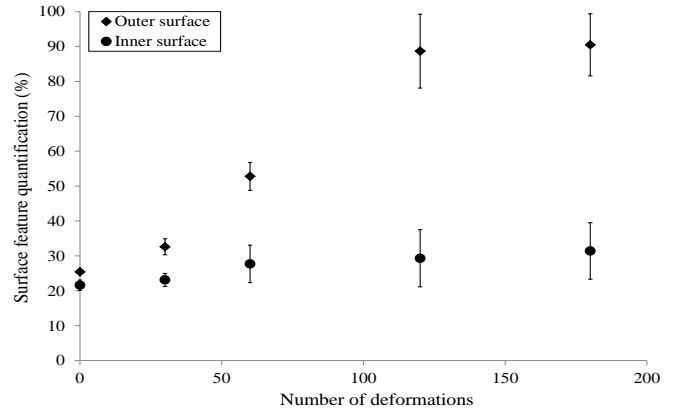

Figure 7. Variation of the proportion of the elastomer surface covered by pores as a function of the number of dynamic biaxial deformations for the NBR-100.
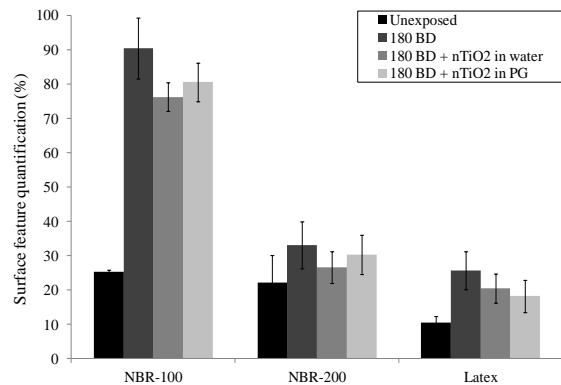

Figure 8. Proportion of the surface covered by pores after 180 BD in the absence or presence of $nTiO_2$ in water or PG. Control samples (no deformations, no colloidal solutions) are also presented for reference.

4. 5. Variation in the Strain Energy

A second mechanical test involved measuring the relative strain energy during each deformation. As shown in Figure 9, an important decrease in the relative strain energy was observed during the first deformations. Thereafter, values reached a plateau, which can be attributed to the Mullins effect. Indeed, some polymer chains reach their limit of extensibility and break during the first deformations, which reduces the energy required to deform the sample during the next cycles [23]. In the absence of the $nTiO_2$ solutions, the variation of the relative strain

5

energy as a function of the number of deformations was similar for the NBR-100 and NBR-200 samples. In the presence of the $nTiO_2$ solutions, the energy required to deform the sample was less important because the elastomer membrane was weakened by its swelling [15]. As it will be shown in section 4.3, NBR-100 swells more than NBR-200 for a similar immersion time, which can explain the difference between plateaus obtained for the two materials, i.e. relative strain energy is low when the swelling of the sample is important. For the NBR-100, results were similar for both solvents (data not shown). On the other hand, for the NBR-200, the variation of the relative strain energy was similar for the $nTiO_2$ in PG and those generated in the absence of the nanoparticles, i.e. the swelling of the NBR-200 that was in contact with the $nTiO_2$ in PG was insignificant. Moreover, only the $nTiO_2$ in water affected the variation of the relative strain energy of latex samples after 80 BD (Figure 10).
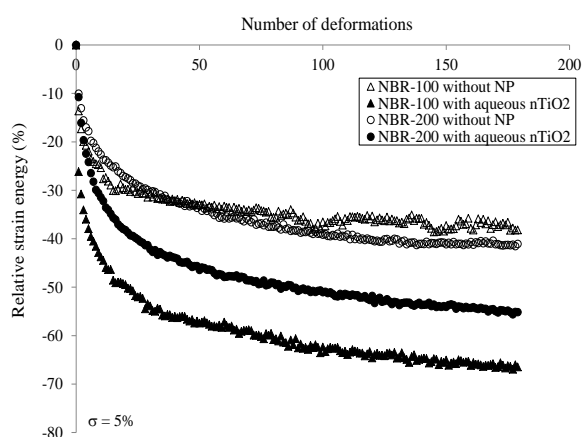

Figure 9. Variation of the relative strain energy as a function of the number of deformations for the NBR-100 and NBR-200 samples in the presence or absence of the aqueous $nTiO_2$.

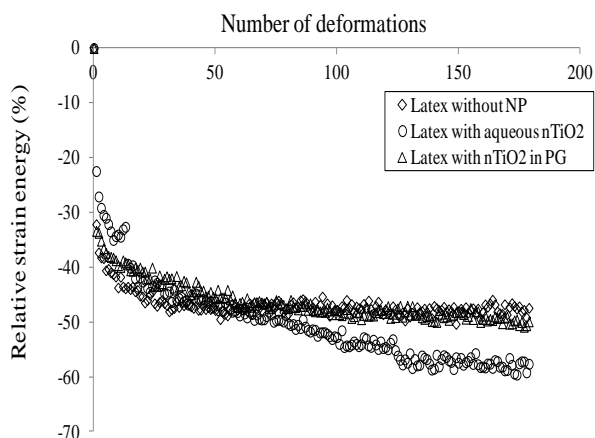

Figure 10. Variation of the relative strain energy as a function of the number of deformations for the latex samples in the presence or absence of $nTiO_2$ solutions.

4. 6. Effect of Mechanical Deformations and the $nTiO_2$ Solutions on the Degree of Crystallinity

Mechanical deformations can lead to a modification in the degree of crystallinity of elastomers [18]. Indeed, the degree of crystallinity (DOC) is a function of the elongation [24]. To highlight this phenomenon, X-ray diffraction was used in order to evaluate the DOC of glove materials that were subjected to mechanical strains in the presence of the $nTiO_2$ solutions. In Figure 11, an X-ray diffraction profile of a native NBR-100 samples and one exposed to 180 BD and aqueous $nTiO_2$ in water. An important decrease in the intensity can be observed after 180 biaxial deformations in presence of the $nTiO_2$ in water.

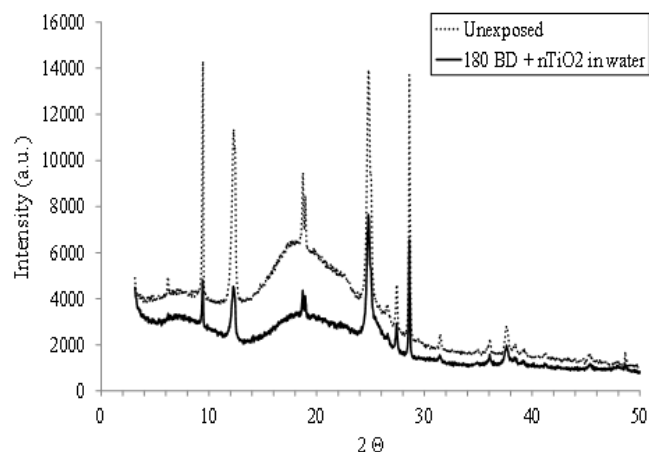Figure 11. X-ray diffraction profile of the native NBR-100 samples and those exposed to 180 BD in the presence of the aqueous $nTiO_2$.

For the NBR-100, the decrease in the degree of crystallinity reached 35% after 180 BD (Figure 12). Complementary XRD analyses showed that the DOC reached this value after only 30 BD (data not shown). As was observed with the strain energy measurements, this decrystallization could be attributed to a polymer chain rupture during the initial deformations, i.e. Mullins effect. The observed decrystallization under stress appeared to be amplified as a result of the contact with the $nTiO_2$ solutions. For example, in the presence of the aqueous $nTiO_2$, the DOC decreased by 44% for the NBR-100 and a similar trend was observed for NBR-200. This increase in the decrystallization could be attributed to plasticisers having leached out of the elastomers when they were swollen by the liquid carrier [25]. This would induce a fragilization of the elastomer chain network after solvent evaporation, which would lead the polymer to become more sensitive to

decrystallization under stress. On the other hand, for latex, the DOC measured appeared to be unaffected by the application of BD.
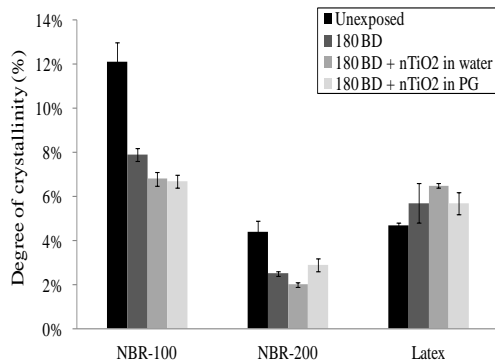

Figure 12. Degree of crystallinity for the three glove materials under four different conditions: unexposed, exposed to 180 biaxial deformations, exposed to 180 biaxial deformations and the aqueous $nTiO_2$ solutions or exposed to 180 biaxial deformations and propylene glycol.

5. Conclusion

Based upon the above results, penetration of nanoparticles through protective glove materials, under conditions simulating occupational use, can attributed in part to a degradation of the physical and mechanical properties of the elastomer that is accelerated by repetitive mechanical deformations and by contact with the $nTiO_2$ solutions. This paper has investigated the physical phenomena behind this facilitated penetration of $nTiO_2$ solutions. To simulate realistic work conditions encountered by protective gloves, one 50% biaxial deformation per minute was applied over 3 hours. It was observed that these dynamical deformations increased the physical degradation of the glove surfaces and decreased the strain energy. Moreover, mechanical deformations with or without the additional contact of the $nTiO_2$ solutions could affect the degree of crystallinity of the elastomer materials. The colloidal solutions had a significant effect on the swelling of both the nitrile rubber and latex glove materials. In conclusion, the results show that great care must be taken in selecting protective gloves for the handling of nanoparticles in colloidal solutions. It is already possible to recommend the frequent replacement of disposable gloves when exposed to $nTiO_2$ in a liquid carrier.

References

[1] B. Hervé-Bazin, (2007) "Les nanoparticules: Un enjeu majeur pour la santé au travail? " EDP Sciences. 704 (in French).

[2] C. O., Robichaud, A. E., Uyar, M. R., Darby, L. G., Zucker, M.R. Wiesner, "Estimates of upper bounds and trends in nano-TiO_2 production as a basis for exposure assessment." Environmental Science and Technology. 43: 2009, p. 4227-4233.

[3] CCHST. (2007) "Basic Information on Titanium Dioxide." [Online]; Available from: http://www.cchst.ca/oshanswers/chemicals/chem_profiles/titanium_dioxide/basic_td.html.

[4] D. Höhr, Y. Steinfartz, R. P. Schins, A. M. Knaapen, G. Martra, B. Fubini, P. J. Borm, "The surface area rather than the surface coating determines the acute inflammatory response after instillation of fine and ultrafine TiO_2 in the rat." International Journal of Hygiene and Environmental Health, 2002. 205(3): p. 239-244.

[5] D. B., Warheit, T. R. Webb, C. M. Sayes, V. L. Colvin, K. L. Reed, "Pulmonary Instillation Studies with Nanoscale TiO_2 Rods and Dots in Rats: Toxicity Is not Dependent upon Particle Size and Surface Area." Toxicological Sciences, 2006. 91(1): p. 227-236.

[6] D. B. Warheit, T. R. Webb, K. L. Reed, S. Frerichs, C. M. Sayes, "Pulmonary toxicity study in rats with three forms of ultrafine-TiO_2 particles: Differential responses related to surface properties. "Toxicology, 2007. 230(1): p. 90-104.

[7] IARC, "Monographs on the evaluation of carcinogenic risks to humans - carbon black, titanium dioxide and talc." 2010, World health organization: Lyon.

[8] C. Ostiguy, B. Roberge, C. Woods, B. Soucy, « Les nanoparticules de synthèse - Connaissances actuelles sur les risques et les mesures de prévention en SST - 2e édition. » 2009, Institut de recherche Robert-Sauvé en santé et en sécurité au travail p. 159 (in French).

[9] OECD, "Current developments/activities on the safety of manufactured nanomaterials - Tour de table at the 7th meeting of the working party on manufactured nanomaterials." in Series on the Safety of Manufactured Manomaterials. 2010: Paris.

[10] L. Golanski, A. Guiot, and F. Tardif, "Are conventional protective devices such as fibrous filter media, respirator cartridges, protective clothing and gloves also efficient for nanoaerosols?" 2008.

[11] L. Golanski, A. Guiot, F. Rouillon, J. Pocachard, F. Tardiff, "Experimental evaluation of personal

protection devices against graphite nanoaerosols: fibrous filter media, masks, protective clothing, and gloves." Human and Experimental Toxicology, 2009. 28(6-7): p. 353-359.

[12] L. Golanski, A. Guoit, and F. Tardif, "Experimental evaluation of individual protection devices against different types of nanoaerosols: graphite, TiO_2 and Pt." Journal of Physics: Conference Series, 2009. 170.

[13] L. Vinches, P. Dolez, K. J. Wilkinson, S. Hallé, "Experimental evaluation of the resistance of nitrile rubber protective gloves against TiO 2 nanoparticles in water under conditions simulating occupational use." Journal of Physics: Conference Series, 2013. 429(1): p. 012056.

[14] L. Vinches, N. Testori, P. Dolez, G. Perron, K. J. Wilkinson, S. Hallé, "Experimental evaluation of the penetration of TiO_2 nanoparticles through protective clothing and gloves under conditions simulating occupational use." Nanoscience Methods, 2013. 2(1): p. 1-15.

[15] L. Vinches, G. Perron, P. Dolez, K. J. Wilkinson, S. Hallé, "Swelling of Elastomers in Solutions of Nanoparticles." ISRN Polymer Science, 2012. 2012: p. 8.

[16] R. F. Domingos, M. A. Baalousha, Y. Ju-Nam, M. M. Reid, N. Tufenkji, J. R. Lead, G. G. Leppard, and K. J. Wilkinson, "Characterizing manufactured nanoparticles in the environment: Multimethod determination of particle sizes." Environmental Science and Technology 2009. 43(19): p. 7277-7284.

[17] L. Harrabi, P. I. Dolez, T. Vu-Khanh, J. Lara, "Evaluation of the flexibility of protective gloves." International Journal of Occupational Safety and Ergonomics, 2008. 14(1): p. 61-68.

[18] J. Marchal, "Cristallisation des caoutchoucs chargés et non chargés sous contrainte:effet sur les chaines amorphes." 2006, Paris XI Orsay: Paris. p. 236 (in French).

[19] J. Runt, and M. Kanchanasopa, "Crystallinity Determination." in Encyclopedia of Polymer Science and Technology. 2002, John Wiley & Sons, Inc.

[20] K. Ahn, and M.J. Ellenbecker, "Dermal and respiratory protection in handling nanomaterials at the center for high-rate nanomanufacturing (CHN)." in AIHce Conference. 2006: Chicago, IL.

[21] L. Vinches, Y, Boulebnane, G. Perron, S. Hallé, P. Dolez, K. J. Wilkinson, "Swelling of Protective Gloves in Commercial TiO_2 Nanoparticles Colloidal Solutions." International Journal of Theoretical and Applied Nanotechnology, 2012. 1(1): p. 45-51.

[22] P. Dolez, L. Vinches, K. Wilkinson, P. Plamdondon, T. Vu-Khanh, "Development of a test method for protective gloves against nanoparticles in conditions simulating occupational use." Journal of Physics: Conference Series, 2011. 304(1): p. 012066.

[23] F. Bueche, "Molecular basis for the mullins effect." Journal of Applied Polymer Science, 1960. 4(10): p. 107-114.

[24] L. E. Alexander, S. Ohlberg, and G. R. Taylor, "X-Ray Diffraction Studies of Crystallization in Elastomers." Journal of Applied Physics, 1955. 26(9): p. 1068-1074.

[25] C. Nohilé, "Étude de l'effet du gonflement par les solvants sur les propriétés du caoutchouc butyle." in Génie mécanique. 2010, École de technologie supérieure: Montréal. p. 201 (in French).